SCIENTIFIC REPORTS
nature research

Check for updates

OPEN

# Effects of nitrogen additions on mesophyll and stomatal conductance in Manchurian ash and Mongolian oak

Kai Zhu[1,2], Anzhi Wang[1], Jiabing Wu[1], Fenghui Yuan[1]✉, Dexin Guan[1]✉, Changjie Jin[1], Yushu Zhang[3] & Chunjuan Gong[1,2]

**The response of plant $CO_2$ diffusion conductances (mesophyll and stomatal conductances, $g_m$ and $g_{sc}$) to soil drought has been widely studied, but few studies have investigated the effects of soil nitrogen addition levels on $g_m$ and $g_{sc}$. In this study, we investigated the responses of $g_m$ and $g_{sc}$ of Manchurian ash and Mongolian oak to four soil nitrogen addition levels (control, low nitrogen, medium nitrogen and high nitrogen) and the changes in leaf anatomy and associated enzyme activities (aquaporin (AQP) and carbonic anhydrase (CA)). Both $g_m$ and $g_{sc}$ increased with the soil nitrogen addition levels for both species, but then decreased under the high nitrogen addition level, which primarily resulted from the enlargements in leaf and mesophyll cell thicknesses, mesophyll surface area exposed to intercellular space per unit leaf area and stomatal opening status with soil nitrogen addition. Additionally, the improvements in leaf N content and AQP and CA activities also significantly promoted $g_m$ and $g_{sc}$ increases. The addition of moderate levels of soil nitrogen had notably positive effects on $CO_2$ diffusion conductance in leaf anatomy and physiology in Manchurian ash and Mongolian oak, but these positive effects were weakened with the addition of high levels of soil nitrogen.**

Nitrogen (N) is an important nutrient for plant photosynthesis because it alters N allocation between photosynthetic components[1], but excessive nitrogen depositions break the soil nitrogen balance and have a strongly negative effect on photosynthesis[2,3]. With global climate change, nitrogen deposition has increased dramatically worldwide[4,5], and its effects on $CO_2$ diffusion conductance (both mesophyll and stomatal conductances, $g_m$ and $g_{sc}$) in photosynthesis have attracted considerable attention in global change, physiological ecology, plant physiology and other fields[6–8]. In contrast to $g_{sc}$, $g_m$ has often been neglected in previous studies, with its supply being assumed to be unlimited[9,10]; the importance of $g_m$ is only being highlighted in recent decades with the advent of advanced instruments and measuring technologies, and studies of $g_m$ have also increased correspondingly[1,11–14].

The relationship of $g_{sc}$ with soil nitrogen has been widely explored; $g_{sc}$ increased with soil nitrogen additions overall[15–17], and $g_m$ also showed a positive correlation with moderate soil nitrogen supplementation in general[1,6,7]. However, excessive nitrogen application resulted in a decrease in the ability to scavenge reactive oxygen species (ROS) in wheat[18]. Many changes under excessive nitrogen application may also occur in photosynthesis electron transport rate ($J_f$) or actual photochemical efficiency of photosystem II ($\Phi_{PS}$ II). In addition, several recent papers also reported that high N conditions reduced evapotranspiration, which resulted in constraining N uptake in almond trees[18–20], and this seemed related to the slight decrease in $g_{sc}$ and leaf N content under high nitrogen condition. Hence, it has not been determined how $g_m$ and $g_{sc}$ responded to excessive nitrogen additions ($\geq$69 kg N $ha^{-1}$ $a^{-1}$). Besides, the changes in leaf anatomy and associated physiological traits were both considered to be important mechanisms in determining $g_m$ and $g_{sc}$[14,21–29].

Xiong *et al.*[14] revealed that leaves with larger $g_m$ in high nitrogen supplement had a larger leaf thickness ($T_{leaf}$) and mesophyll surface area exposed to intercellular space per unit leaf area ($S_{mes}$) than those in low nitrogen supplementation, and Zhu *et al.*[30] also showed that $T_{leaf}$ and mesophyll cell thickness ($T_{mes}$) both imposed a positive

[1]Key Laboratory of Forest Ecology and Management, Institute of Applied Ecology, Chinese Academy of Sciences, Shenyang, 110016, China. [2]University of Chinese Academy of Sciences, Beijing, 100049, China. [3]The Institute of Atmospheric Environment, China Meteorological Administration, Shenyang, 110166, China. ✉e-mail: fhyuan@iae.ac.cn; dxguan@iae.ac.cn

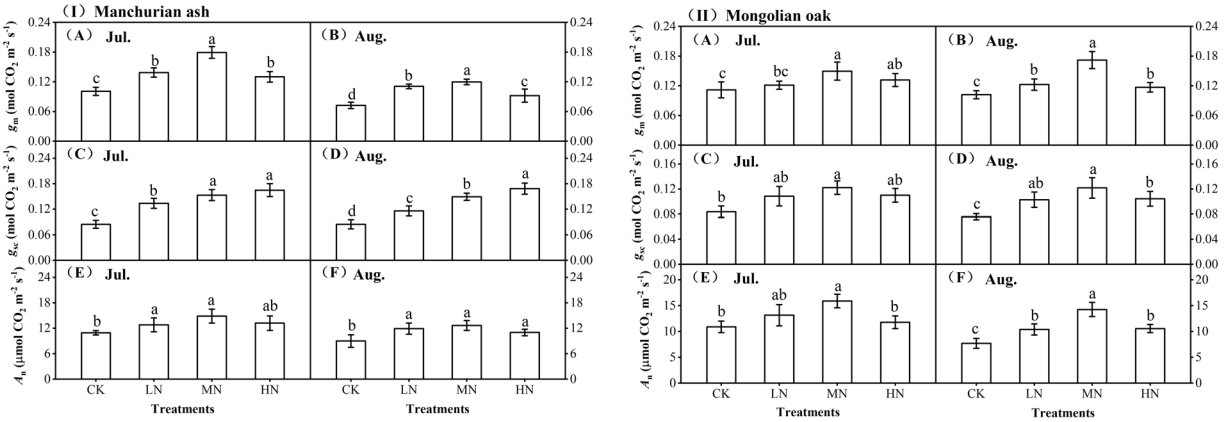


**Figure 1.** Changes of plant $g_m$, $g_{sc}$ and $A_n$ with soil N additions in Manchurian ash (I) and Mongolian oak (II) in July and August. Values were means ± SE (n = 5), and different lowercase letters (**a**–**c**) indicated significant difference at $P < 0.05$. CK, the control; LN, low nitrogen addition; MN, medium nitrogen addition; HN, high nitrogen addition.

effect on $g_m$ recovery in Manchurian ash and Mongolian oak, while $S_{mes}$ had a negative effect on this parameter. In addition, Xiong *et al.*[29] and Zhu *et al.*[30] both revealed the determination of stomatal features (size and density) and opening status (SS) to $g_{sc}$, and Zhu *et al.*[30] suggested a positive correlation between SS and $g_{sc}$ in Manchurian ash and Mongolian oak, which was also supported by the study of Xu and Zhou (2008)[31]. Besides, the changes of $g_m$ and $g_{sc}$ would also be significantly affected by aquaporin (AQP) and carbonic anhydrase (CA) activities[14,21]. AQP mediates the genes in the plasma membrane intrinsic protein (PIP) aquaporin family, and its increase in activity strongly promotes the expression of PIPs and improves $CO_2$ membrane permeability[32–34]. CA regulates $g_m$ mainly by changing the dynamics of $CO_2$ to $^-HCO_3$[28]. However, it has not been determined how leaf anatomies and AQP and CA activities would change in the Changbai Mountains with the addition of various levels of soil nitrogen.

Manchurian ash (*Fraxinus mandshurica* Rupr.) and Mongolian oak (*Quercus mongolica* Fish. ex Ledeb), two species in Oleaceae and Fagaceae, respectively, are widely distributed in the Changbai Mountains, China. Their responses of $CO_2$ diffusion conductance to soil nitrogen additions have rarely been reported; and the mechanisms governing $g_m$ and $g_{sc}$ in leaf anatomy and physiology have not been determined. Hence, we measured both $g_m$ and $g_{sc}$ and their related anatomical and physiological traits, including leaf N content and AQP and CA activities, to explore the responses of $CO_2$ diffusion conductance to the addition of various levels of soil nitrogen. The present study will advance our mechanistic understanding of global nitrogen deposition impacts on carbon cycling in tree species.

## Results

**Effects of soil nitrogen additions on $g_m$.** Considerable changes in $g_m$ were observed in both species after soil nitrogen addition compared with the control values (CK) (Fig. 1a,b). The $g_m$ gradually increased with the addition of various levels of soil nitrogen, reaching the maximum with the medium level of 46 kg N $ha^{-1}$ $a^{-1}$ (MN) and then decreasing with the addition of 69 kg N $ha^{-1}$ $a^{-1}$ (HN) while remaining greater than the $g_m$ observed for the CK group. Overall, $g_m$ showed significant differences among the four nitrogen-addition treatments in both species, in which it was significantly larger in the MN treatment than in the other treatments ($P < 0.05$). In addition, the $g_m$ in August was slightly lower than that in July in both species overall.

**Effects of soil nitrogen additions on $g_{sc}$.** Concurrently, soil nitrogen addition also resulted in a significant increase in $g_{sc}$, with a different trend being observed between Manchurian ash and Mongolian oak (Fig. 1c,d). In Manchurian ash, $g_{sc}$ continued to increase with nitrogen addition in July and August, but it increased from low nitrogen (LN, 23 kg N $ha^{-1}$ $a^{-1}$) to MN and then decreased with the addition of HN in Mongolian oak. The $g_{sc}$ with the nitrogen addition treatments was significantly larger than that of the control values in July and August in both species ($P < 0.05$). Overall, the $g_{sc}$ in Manchurian ash was considerably larger than that in Mongolian oak. In addition, influenced by the changes in $g_m$ and $g_{sc}$, leaf $A_n$ also increased first and then decreased with the addition of progressively higher levels of soil nitrogen (Fig. 1e,f), indicating that plant photosynthetic capacities could also be considerably strengthened by soil nitrogen additions.

**Effects of soil nitrogen addition on leaf anatomical characteristics.** *Effects on mesophyll anatomical traits.* The addition of soil nitrogen caused some changes in mesophyll anatomical traits (Table 1), including leaf ($T_{leaf}$) and mesophyll cells ($T_{mes}$) thicknesses, the surface area of mesophyll cells exposed to intercellular space ($S_{mes}$) and the ratio of mesophyll surface ($A_{mes}$) to total leaf surface area ($A_T$) corrects for the actual area available for $CO_2$ diffusion ($A_T/A_{mes}$). $T_{leaf}$, $T_{mes}$, $S_{mes}$ and $A_T/A_{mes}$ all increased after soil nitrogen addition in overall without $T_{leaf}$ in HN and $A_T/A_{mes}$ in LN treatment and were lower than the CK values. When nitrogen supplementation was no more than 69 kg N $ha^{-1}$ $a^{-1}$, $T_{leaf}$ and $S_{mes}$ increased with nitrogen addition in both species, and $T_{mes}$ also showed increases with the addition of soil nitrogen in Manchurian ash and reached a maximum in the MN treatment, while it reached a maximum in the LN treatment in Mongolian oak. Significant differences between

| | Manchurian ash | | | | | | Mongolian oak | | | | | |
|---|---|---|---|---|---|---|---|---|---|---|---|---|
| | $T_{leaf}$ (μm) | $T_{mes}$ (μm) | $S_{mes}$ (μm$^2$ μm$^{-2}$) | $A_T/A_{mes}$ | $g_{ias}$ ($10^{-2}$ m s$^{-1}$) | $g_{liq}$ ($10^{-4}$ m s$^{-1}$) | $T_{leaf}$ (μm) | $T_{mes}$ (μm) | $S_{mes}$ (μm$^2$ μm$^{-2}$) | $A_T/A_{mes}$ | $g_{ias}$ ($10^{-2}$ m s$^{-1}$) | $g_{liq}$ ($10^{-4}$ m s$^{-1}$) |
| CK | $130.1 \pm 11.0^{bc}$ | $116.3 \pm 5.1^{bc}$ | $12.1 \pm 2.0^{a}$ | $1.91 \pm 0.08^{ab}$ | $4.47 \pm 0.37^{d}$ | $1.08 \pm 0.06^{b}$ | $206.8 \pm 3.2^{bc}$ | $158.1 \pm 6.7^{c}$ | $12.9 \pm 1.3^{b}$ | $1.81 \pm 0.11^{a}$ | $5.41 \pm 0.33^{c}$ | $1.14 \pm 0.06^{b}$ |
| LN | $135.9 \pm 5.1^{b}$ | $122.9 \pm 4.2^{ab}$ | $14.2 \pm 3.8^{a}$ | $1.74 \pm 0.11^{b}$ | $11.93 \pm 0.79^{a}$ | $1.19 \pm 0.14^{ab}$ | $213.7 \pm 4.7^{b}$ | $185.9 \pm 3.5^{a}$ | $13.0 \pm 1.5^{ab}$ | $1.67 \pm 0.40^{a}$ | $6.21 \pm 0.42^{b}$ | $1.24 \pm 0.12^{ab}$ |
| MN | $148.2 \pm 7.3^{a}$ | $130.2 \pm 2.5^{a}$ | $15.2 \pm 2.6^{a}$ | $2.35 \pm 0.53^{a}$ | $10.13 \pm 0.74^{b}$ | $1.28 \pm 0.05^{a}$ | $227.4 \pm 6.0^{a}$ | $171.2 \pm 8.0^{b}$ | $16.0 \pm 2.0^{a}$ | $1.85 \pm 0.34^{a}$ | $7.22 \pm 0.22^{a}$ | $1.32 \pm 0.07^{a}$ |
| HN | $122.9 \pm 3.6^{c}$ | $112.9 \pm 3.3^{c}$ | $18.0 \pm 5.0^{a}$ | $2.43 \pm 0.16^{a}$ | $8.11 \pm 1.03^{c}$ | $1.06 \pm 0.07^{b}$ | $202.9 \pm 2.4^{c}$ | $167.1 \pm 4.1^{bc}$ | $14.4 \pm 1.7^{ab}$ | $1.78 \pm 0.22^{a}$ | $5.76 \pm 0.59^{bc}$ | $1.17 \pm 0.04^{b}$ |

**Table 1.** Values of leaf anatomical characteristics for different nitrogen addition treatments in Manchurian ash and Mongolian oak. All data were means ± SE (n = 5). Different lowercase letters (a, b, c) indicated significant differences between nitrogen addition treatments at $P < 0.05$. CK, the control; LN, low nitrogen addition; MN, medium nitrogen addition; HN, high nitrogen addition.

| | Manchurian ash | | | | Mongolian oak | | | |
|---|---|---|---|---|---|---|---|---|
| | PL (μm) | PW (μm) | SS (μm$^2$) | $D_s$ ($10^{-2}$ N cm$^{-2}$) | PL (μm) | PW (μm) | SS (μm$^2$) | $D_s$ ($10^{-2}$ N cm$^{-2}$) |
| CK | $7.01 \pm 0.70^{b}$ | $3.04 \pm 0.97^{ab}$ | $17.57 \pm 1.72^{b}$ | $6.32 \pm 0.45^{b}$ | $6.36 \pm 0.52^{a}$ | $2.47 \pm 0.58^{b}$ | $12.78 \pm 1.15^{b}$ | $9.48 \pm 0.45^{b}$ |
| LN | $7.26 \pm 0.14^{ab}$ | $3.18 \pm 0.27^{a}$ | $18.10 \pm 1.43^{ab}$ | $8.28 \pm 0.94^{a}$ | $6.53 \pm 0.19^{a}$ | $2.54 \pm 0.35^{b}$ | $13.06 \pm 2.20^{b}$ | $11.89 \pm 0.69^{a}$ |
| MN | $7.66 \pm 0.19^{a}$ | $3.28 \pm 0.27^{a}$ | $19.74 \pm 2.11^{a}$ | $8.43 \pm 1.14^{a}$ | $6.71 \pm 0.30^{a}$ | $3.13 \pm 0.12^{a}$ | $16.52 \pm 1.42^{a}$ | $11.14 \pm 0.26^{a}$ |
| HN | $7.35 \pm 0.05^{ab}$ | $2.73 \pm 0.13^{b}$ | $15.74 \pm 0.68^{b}$ | $9.93 \pm 0.90^{a}$ | $6.25 \pm 0.29^{a}$ | $2.40 \pm 0.19^{b}$ | $11.81 \pm 1.51^{b}$ | $9.63 \pm 0.69^{b}$ |

**Table 2.** Values of stomatal parameters for different nitrogen addition treatments in Manchurian ash and Mongolian oak. All data were means ± SE (n = 64). Different lowercase letters (a, b, c) indicated significant differences between nitrogen addition treatments at $P < 0.05$. SS, stomatal opening status; PL and PW, stomatal pore length and width at the centre of the stoma; $D_s$, stomatal density. CK, the control; LN, low nitrogen addition; MN, medium nitrogen addition; HN, high nitrogen addition.

| | Manchurian ash | | Mongolian oak | |
|---|---|---|---|---|
| | July | August | July | August |
| CK | $13.1 \pm 0.88^{ab}$ | $10.4 \pm 0.31^{b}$ | $13.0 \pm 1.22^{b}$ | $10.2 \pm 0.93^{b}$ |
| LN | $14.4 \pm 0.83^{b}$ | $11.8 \pm 0.55^{a}$ | $16.4 \pm 3.05^{ab}$ | $15.7 \pm 2.73^{a}$ |
| MN | $15.2 \pm 0.46^{a}$ | $11.9 \pm 0.32^{a}$ | $19.1 \pm 1.12^{a}$ | $15.5 \pm 0.47^{a}$ |
| HN | $15.0 \pm 1.85^{ab}$ | $11.1 \pm 1.10^{ab}$ | $16.0 \pm 1.48^{ab}$ | $12.8 \pm 0.93^{ab}$ |

**Table 3.** Values of leaf N content (g kg$^{-1}$) during soil nitrogen additions in July and August in both species. All values were means ± SE (n = 3). Different lowercase letters (a, b, c) indicated significant differences between nitrogen addition treatments at $P < 0.05$. CK, the control; LN, low nitrogen addition; MN, medium nitrogen addition; HN, high nitrogen addition.

nitrogen addition treatments were observed in $T_{leaf}$ and $T_{mes}$, while no significant differences were shown for $S_{mes}$ and $A_T/A_{mes}$ overall in both species ($P < 0.05$).

*Changes of leaf $g_{ias}$ and $g_{liq}$.* Changes of $T_{mes}$ and $A_T/A_{mes}$ to soil nitrogen additions also directly caused changes in leaf gas-phase ($g_{ias}$) and liquid-phase $CO_2$ diffusion conductance ($g_{liq}$) inside mesophyll cells (Table 1). Both $g_{ias}$ and $g_{liq}$ gradually increased with MN and then decreased under HN treatment. A significant difference between nitrogen addition treatments was observed in $g_{ias}$, while $g_{liq}$ did not change significantly overall ($P < 0.05$).

*Effects on stomatal parameters.* Correspondingly, soil nitrogen addition also caused considerable changes in stomatal parameters, mainly including stomatal pore length and width at the centre of the stoma (PL and PW), stomatal opening status (SS) and density ($D_s$) (Table 2). As two important components to SS, PL and PW both increased with the MN treatment and were similar in both species, but in the HN treatment, they both fell below the CK values. Consequently, leaf SS gradually increased with soil nitrogen addition and then significantly decreased to a minimum under HN treatment. Besides, significant increases also happened to leaf $D_s$ after soil nitrogen additions ($P < 0.05$) (Table 2), in which Manchurian ash showed a gradually increased $D_s$ with soil nitrogen addition, reaching the maximum under HN treatment, while $D_s$ increased first then decreased in Mongolian oak, reaching its maximum under LN treatment.

**Effects of soil nitrogen additions on leaf N content.** Changes in leaf N content in both species during soil nitrogen additions are shown in Table 3. The leaf N content was enlarged by soil nitrogen addition and increased with medium nitrogen addition to MN and then decreased under HN treatment. Overall, no significant differences in leaf N content between soil nitrogen addition treatments were observed in both species

| | Manchurian ash | | Mongolian oak | |
|---|---|---|---|---|
| | AQP (U $g^{-1}$) | CA (U $g^{-1}$) | AQP (U $g^{-1}$) | CA (U $g^{-1}$) |
| CK | $5.57 \pm 0.29^{b}$ | $1.54 \pm 0.09^{a}$ | $5.57 \pm 0.15^{c}$ | $1.42 \pm 0.10^{ab}$ |
| LN | $5.78 \pm 0.09^{ab}$ | $1.57 \pm 0.05^{a}$ | $6.00 \pm 0.11^{b}$ | $1.40 \pm 0.03^{ab}$ |
| MN | $5.92 \pm 0.04^{a}$ | $1.64 \pm 0.08^{a}$ | $6.80 \pm 0.06^{a}$ | $1.51 \pm 0.02^{a}$ |
| HN | $5.91 \pm 0.13^{a}$ | $1.61 \pm 0.09^{a}$ | $6.17 \pm 0.31^{b}$ | $1.38 \pm 0.03^{b}$ |

**Table 4.** Values of leaf AQP and CA activities during soil nitrogen additions in both species. All values were means ± SE (n = 3). Different lowercase letters (a, b, c) indicated significant differences between nitrogen addition treatments at $P < 0.05$. CK, the control; LN, low nitrogen addition; MN, medium nitrogen addition; HN, high nitrogen addition.

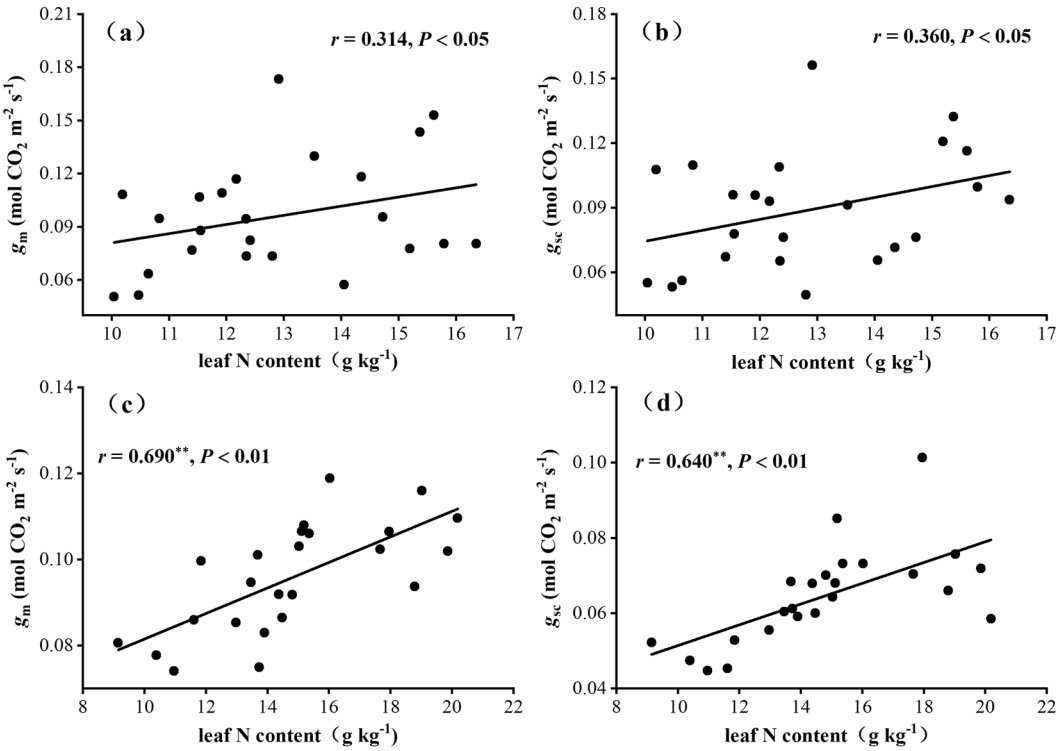


**Figure 2.** The correlations between $g_m$, $g_{sc}$ and leaf N content in Manchurian ash (**a**,**b**) and Mongolian oak (**c**,**d**). The coefficient of correlation ($r$) and significant correlation were at $P < 0.05$ and $^{**}P < 0.01$.

($P < 0.05$), and Mongolian oak saplings maintained a higher leaf N content in nitrogen addition treatments than did Manchurian ash saplings.

**Effects of soil nitrogen addition on AQP and CA activities.** Soil nitrogen addition also had great effects on leaf AQP and CA activities in both species (Table 4). In this study, the activities of AQP and CA were both enlarged after soil nitrogen addition, and they also gradually strengthened with soil nitrogen added to MN and then weakened with the HN treatment. Similarly, the activities of these two enzymes also did not show significant differences between the four nitrogen addition treatments overall ($P < 0.05$).

## Discussion

**Increases in $g_m$ and $g_{sc}$ mostly resulted from the improvement of leaf N content.** Our results showed that both $g_m$ and $g_{sc}$ were enlarged by soil nitrogen addition; specifically, these values increased with nitrogen addition from LN to MN and then decreased with the addition of HN. Concurrently, leaf N content also presented a similar change with soil nitrogen addition (See Table 3). We believed that the increases of $g_m$ and $g_{sc}$ were largely related to the enlargement of leaf N content in this study because the relationships between leaf N content and $g_m$ and $g_{sc}$ strongly supported the promotion of leaf N content to $g_m$ and $g_{sc}$ increases, in which $g_m$ and $g_{sc}$ both showed a positive correlation with leaf N content, even though they were highly significant in Mongolian oak ($P < 0.01$) (Fig. 2). This finding was supported by the positive links between leaf N content and $CO_2$ diffusion conductance (both $g_m$ and $g_{sc}$) in studies of Li *et al.*[6] and Yamori *et al.*[1].

The positive correlation between leaf N content and $g_m$ found in the current study supported earlier observations that if leaves were treated individually, leaf N content explained 32% of measured variability in $A_n$ but only 11% of that in $g_m$, while variation in $g_m$ explained 33% of variation in $A_n$[47]. With three-quarters of leaf N associated with photosynthesis (mostly Rubisco and chlorophyll), the relationship between N and $g_m$ might simply reflect the relationship between $A_n$ and $g_m$[48]. In this study, leaf N content increased under soil nitrogen addition conditions (Table 3), this made great improvements to leaf photosynthetic capacity and $g_m$ (from CK to MN, see Fig. 1), but the excessive N supply (high N addition of 69 kg N $ha^{-1}$ $a^{-1}$, HN) would lower Rubisco activity and content, $g_m$ and $C_c$[49].

On the other hand, the release of photorespiratory $CO_2$ occurred in the bundle-sheath mitochondria might make an enriched $CO_2$ partial pressure in the bundle-sheath chloroplast in $C_3$ species and result in an increased amount of $CO_2$ to be refixed by Rubisco[50–53]. The amount of (photo)respiratory $CO_2$ that was refixed by Rubisco can be calculated from the diffusion resistances[54]. The $g_m$, as an apparent conductance, could also be strongly affected by respiratory and photorespiratory $CO_2$ diffusing towards the chloroplasts from the mitochondria[54]. In this study, both $CO_2$ compensation point in the absence of respiration ($\Gamma^*$) and the mitochondrial respiration in the light ($R_d$) differed among nitrogen addition levels in Manchurian ash and Mongolian oak (Table S2). This difference might enrich $CO_2$ partial pressure in the bundle-sheath chloroplast in Manchurian ash and Mongolian oak, and increase the amount of $CO_2$ refixed by Rubisco, finally making large influences on $g_m$ responding to soil nitrogen additions. However, $\Gamma^*$ and $R_d$ did not show significant declines under high nitrogen addition condition as other gas exchange parameters (Table S2). This might be due to the bias of the Laisk method in the estimation $\Gamma$*. The Laisk method was pointed out that what it estimated is the intercellular $CO_2$ partial pressure ($C_i^*$), rather than the true $CO_2$ photocompensation point[14,54]. In other words, the $\Gamma^*$ measured in the current study might be the $C_i^*$ actually, and this would lead to an enlarged $CO_2$ photocompensation point under high nitrogen addition condition, but this only held under the assumption of combined resistance of chloroplast envelope and stroma ($r_{ch}$) being negligible. If $r_{ch}$ made up a significant portion of mesophyll resistance ($r_m$), the $C_i^*$ was no longer necessarily smaller than the true $\Gamma^*$; it might be equal to $\Gamma^*$, or even greater[54]. Hence, the $\Gamma^*$ value estimated using the classical Laisk method and its response to soil N supplement might exist uncertainties under high or excessive nitrogen addition condition.

Since a positive relationship between leaf N content and $CO_2$ assimilation was reported in numerous studies in which N increased Rubisco content and activity[1,6,55–59], the positive effect of leaf N content on $g_m$ and $g_{sc}$ might also be achieved, as it improved the activities of related enzymes, such as AQP and CA[28,30,33], which had been implicated in regulation of $g_m$[48,60]. In this study, the activities of AQP and CA were strengthened by soil nitrogen addition (Table 4). This would largely promote the expression of genes greatly in the plasma membrane intrinsic protein (PIP) aquaporin family[34]. Furthermore, the diffusion of $CO_2$ in mesophyll cells was not only a complexly physical process, but also a chemical reaction process[10]. The improvements of AQP and CA activities under nitrogen addition could stimulate the chemical reactions by improving the conversion of $CO_2$ to $^-HCO_3$ and the membrane permeabilities to $CO_2$ at plasma membrane, cytosol and chloroplast stroma in mesophyll cells[28,32,61]. Additionally, nitrogen addition could also promote AQP gene expressions, like the PIP2 aquaporin gene family[62,63], which benefited $CO_2$ transmembrane transport and consequently increase $g_m$[14]. Hence, the nitrogen addition in this study might result in an increased $CO_2$ permeability in oocytes membranes expressing *Nt*AQP1[64], eventually leading to the enhancements of $g_{liq}$ and $g_m$.

**Strong promotion of soil nitrogen addition on $g_m$ and $g_{sc}$, as explained in leaf anatomy.** In this study, leaf anatomical structures were adjusted by soil nitrogen additions from the changes in anatomical characteristics (See Tables 1 and 2), which exhibited notably positive effects on $g_m$ and $g_{sc}$, as leaf anatomical structures were tightly correlated with $g_m$ and $g_{sc}$[14,26,56,61–63]. Furthermore, as two stages in $CO_2$ diffusion, the gas- and liquid-phase diffusional processes were largely strengthened in nitrogen addition leaves, as suggested by the increases of $g_{ias}$ and $g_{liq}$ (See Table 1). However, $g_{ias}$ and $g_{liq}$ in the high nitrogen addition treatment were lower than those in the low and medium nitrogen addition treatments (LN and MN) in Manchurian ash and Mongolian oak, which was in keeping with the results obtained for rice in Li *et al.*[6].

Both $T_{leaf}$ and $T_{mes}$ increased with soil nitrogen added to MN level and then decreased with the addition of HN (See Table 1); these treatments enlarged total leaf ($A_T$) and mesophyll surface areas ($A_{mes}$) for the actual areas available for $CO_2$ diffusion (data not shown), widened $CO_2$ flow pathways[44,56], and correspondingly enlarged $g_{ias}$. However, $g_{ias}$ was often suggested to be the minor component to $g_m$, while $g_{liq}$ was the major one[38,42,64]. Hence, suggested by our previous conclusion that the recovery of $g_m$ after soil rewatering was mainly resulted from the increase of $g_{liq}$ in Zhu *et al.*[30], we believed the important promotion of soil nitrogen addition on $g_m$ increase in this study would also be reached from the enlargement in $g_{liq}$. The $g_{liq}$ is tightly related to $S_{mes}$, cell wall thickness ($T_{cw}$) and the chloroplast surface facing the intercellular space per unit leaf area ($S_c$)[24,26,42,65]. The increase of $S_{mes}$ in this study (See Table 1) enlarged the touching area between $CO_2$ and mesophyll cells and then improved the efficiency of $CO_2$ transmembrane diffusion. Although we did not measure $T_{cw}$ and $S_c$, the $S_c$ should be enlarged, while $T_{cw}$ decreased, by soil nitrogen addition in this study, as $S_c$ had been revealed to increase with nitrogen supply in rice[14], and $T_{cw}$ was negative with both $S_c$ and $g_m$[66,67]. The changes in $S_c$ and $T_{cw}$ would also strongly promote increased $g_m$. Finally, the increase of $A_T/A_{mes}$ caused by mesophyll anatomical changes directly resulted in the enlargement of $g_{liq}$. In addition, leaf PL and PW were enlarged by soil nitrogen additions in both species (See Table 2), which resulted in the improvement of stomatal opening status (SS) and broadened $CO_2$ diffusion pathway from leaf surface to substomatal cavities. Since Xiong *et al.*[29] suggested that the change of SS would affect $g_{sc}$ in leaf anatomy, the enlargement of SS in this study would largely promote the increase of $g_{sc}$ in both species.

In summary, our data showed a different effect of soil nitrogen addition levels on leaf anatomical characteristics in this study, which reached the maximum under MN treatment and decreased under the addition of HN, indicating a decreased positive effect from high soil nitrogen addition on plant metabolism. In addition, soil

nitrogen addition could decrease the distance between the intercellular space and catalytic site of Rubisco ($D_{I\text{-}R}$) and markedly could increase chloroplast size, finally facilitating $CO_2$ diffusion in the liquid phase of mesophyll cells[6,68]. This phenomenon would be another important aspect to explain the effect of leaf anatomy on $g_m$ during soil nitrogen addition.

## Conclusion

Soil nitrogen additions could enlarge $CO_2$ diffusion conductance (both $g_m$ and $g_{sc}$) markedly in Manchurian ash and Mongolian oak in Changbai Mountains, but its promotion was dependent on the addition levels. Moderate soil nitrogen additions ($\leq$46 kg N $ha^{-1}$ $a^{-1}$) increased $g_m$ and $g_{sc,}$ and they reached their maximum under the addition of 46 kg N $ha^{-1}$ $a^{-1}$, but this positive effect was weakened with the addition of high level of 69 kg N $ha^{-1}$ $a^{-1}$. The effects of soil nitrogen addition on $g_m$ and $g_{sc}$ mostly resulted from improvements in physiological traits, such as leaf N content and the activities of AQP and CA, and adjustments in anatomical characteristics, including $T_{leaf}$, $T_{mes}$, $S_{mes}$ and stomatal opening status.

## Material and methods

**Plant material and experimental design.** Five-year-old potted saplings of similar size in Manchurian ash and Mongolian oak were selected as the materials at the National Research Station of Changbai Mountain Forest Ecosystems of the Chinese Academy of Sciences located in Jilin province of northeast China (128°06′E, 42°24′N), and they were transplanted into individual pots in 2015, filled with 27 l soils collected from a broad-leaved Korean pine forest with a mean annual nitrogen forest deposition of 23 kg N $ha^{-1}$ $a^{-1}$. The roots in the pots were blocked from the outside soil by the pedestals placed under the pots. The volume of the pots was 29.28 L with a height of 30.0 cm and a diameter of 34.3 cm.

Four nitrogen addition levels were used to simulate nitrogen deposition intensities with the addition of no nitrogen (CK), low nitrogen (LN, 23 kg N $ha^{-1}$ $a^{-1}$), medium nitrogen (MN, 46 kg N $ha^{-1}$ $a^{-1}$) and high nitrogen (HN, 69 kg N $ha^{-1}$ $a^{-1}$). Urea solutions with different concentrations of nitrogen were sprayed into the pots once every other month from May to October in 2017. Five replicates were designed for each treatment, and all potted saplings were thoroughly watered daily to avoid water deficit. All measurements were carried out during summer growth season (July and August) to explore the changes in effects of soil nitrogen addition on $g_m$ and $g_{sc}$.

**Simultaneous gas exchange and chlorophyll fluorescence measurements.** We simultaneously measured gas exchange and chlorophyll fluorescence on newly and fully expanded, sun-exposed leaves using an open-flow gas exchange system (Li-6400XT; Li-Cor Inc., Lincoln, NE, USA) equipped with an integrated fluorescence leaf chamber (Li-6400-40; Li-Cor). Leaves were fully light adopted under a saturated photosynthetic active photon flux density (PPFD) of 1200 μmol $m^{-2}$ $s^{-1}$ provided by Li-6400 with a 10: 90 blue: red light for 30 minutes, while leaf temperature and relative humidity and $CO_2$ concentration in the leaf chamber were maintained at 25 °C and 60 ± 5% and 400 μmol $CO_2$ $mol^{-1}$ with a $CO_2$ mixture, respectively. In addition, the gas flow rate was controlled at 300 μmol $s^{-1}$ to ensure the adequate gas exchange. After stabilization to a steady state, gas exchange parameters, steady-state fluorescence ($F_s$) and maximum fluorescence ($F_m'$) were recorded.

The actual photochemical efficiency of photosystem II ($\Phi_{PS}$ II) was calculated according to Genty *et al.*[35]:

$$\Phi_{PSII} = \frac{(F'_m - F_s)}{F'm} \quad (1)$$

The photosynthesis electron transport rate ($J_f$) was calculated as follows:

$$J_f = \Phi_{PSII} \cdot PPFD \cdot \alpha\beta \quad (2)$$

where $\alpha$ is the total leaf absorptance and $\beta$ is the partitioning of absorbed quantum between PS II and PS I.

In this study, light response curves ($A_n$-PPFD curve) for controlled and nitrogen-addition saplings were also measured under a low $O_2$ concentration (<1%) condition to correct the $\alpha\beta$, as it was equal to the slope of the relationship between $\Phi_{PS}$ II and $4\Phi_{CO2}$ (the quantum efficiency of $CO_2$ fixation)[36]. Values of $\alpha\beta$ for different nitrogen treatments were shown in Table S1.

The mesophyll conductance ($g_m$) was calculated using the 'variable *J* method' described in Harley *et al.*[37]:

$$g_m = \frac{A_n}{C_i - \frac{\Gamma^*(J_f + 8(A_n + R_d))}{J_f - 4(A_n + R_d)}} \quad (3)$$

where $A_n$ is the net photosynthetic rate, $C_i$ is the intercellular $CO_2$ concentration, and these values were directly obtained from gas exchange measurements; $\Gamma^*$ represents the $CO_2$ compensation point in the absence of respiration and $R_d$ represents the mitochondrial respiration in the light.

$\Gamma^*$ and $R_d$ were measured using the Laisk method, namely, 5 initial slopes of $A_n$-$C_i$ curves under low light and low $CO_2$ concentrations were measured for $\Gamma^*$ and $R_d$ estimations in this study[38,39]. In theory, three $CO_2$ response curves obtained by varying $CO_2$ concentrations from 150 to 40 μmol $CO_2$ $mol^{-1}$ under three PPFDs (150, 100 and 50 μmol $m^{-2}$ $s^{-1}$) would intersect with each other at a point, and the intersection point at *x*-axis and *y*-axis were considered to $\Gamma^*$ and $R_d$, respectively. But in practice, these three linear regressions of the intersected $A_n$-$C_i$ curves formed a triangle range rather than a single point[40] (Fig. S1), and the $\Gamma^*$ and $R_d$ were calculated as the barycenter of the triangle formed by the intersection of the three lines at *x*-axis and *y*-axis, respectively, according to our previous published method[40]. The values of $\Gamma^*$ and $R_d$ during soil nitrogen additions were shown in Table S2.

Stomatal conductance to $CO_2$ ($g_{sc}$, mol $CO_2$ $m^{-2}$ $s^{-1}$) was calculated from the ratio of stomatal conductance to water ($g_{sw}$, mol $CO_2$ $m^{-2}$ $s^{-1}$) to 1.6 (i.e., $g_{sc} = g_{sw}/1.6$), as $g_{sw}$ was 1.6 times larger than $g_{sc}$[41].

**Measurement of leaf anatomical characteristics.** After gas exchange measurements, we cut fifteen small leaf samples (4.0 mm × 1.5 mm) from five replicated leaves per treatment and fixed them in FAA (alcohol: formaldehyde: glacial acetic acid = 90: 5: 5) to measure leaf anatomical characteristics, mainly including leaf thickness ($T_{leaf}$, μm), mesophyll and stomatal anatomical characteristics, such as the thickness of mesophyll cells between the two epidermal layers ($T_{mes}$, μm) and the surface area of mesophyll cells exposed to intercellular space per unit leaf area ($S_{mes}$, $\mu m^2\ \mu m^{-2}$) calculated using formula (4), stomatal pore length (PL, μm) and width (PW, μm) at the centre of the stoma, which were detailed described in Zhu *et al.*[30]. Besides, we counted the number of stomata per unit leaf area to calculate the stomatal density ($D_s$, N $cm^{-2}$).

$$S_{mes} = \frac{L_{mes}}{W} \cdot F \tag{4}$$

where the length of mesophyll cells exposes to intercellular space ($L_{mes}$, μm) and the cross-sectional width ($W$, μm) are measured with Image J software. The curvature correction factor ($F$) was measured using the method described in the study of Evans *et al.*[42] and Thain (1983)[43], which was shown in Table S3.

We also calculated the gas- and liquid-phase $CO_2$ diffusion conductance in mesophyll cells (i.e., $g_{ias}$ and $g_{liq}$) with leaf anatomical characteristics according to formulas (5) and (6) to assess their relationships with $g_m$.

$$g_{ias} = \frac{D_a f_{ias}}{\Delta L_{ias} \varsigma} \tag{5}$$

$$\frac{1}{g_{liq}} = \left(\frac{1}{g_{cw}} + \frac{1}{g_{pl}} + \frac{1}{g_{ct}} + \frac{1}{g_{en}} + \frac{1}{g_{st}}\right)\frac{A_T}{A_{mes}} \tag{6}$$

where $D_a$ ($m^2\ s^{-1}$) is the diffusion coefficient for $CO_2$ in the gas phase, $\Delta L_{ias}$ (μm) is taken as half $T_{mes}$[26,44], ς is the diffusion path tortuosity (m $m^{-1}$) and $f_{ias}$ (%) is the fraction of mesophyll volume occupied by the intercellular airspace. $g_{cw}$, $g_{pl}$, $g_{ct}$, $g_{en}$ and $g_{st}$ are the partial conductance for the cell wall, plasmalemma, cytosol, chloroplast envelope and chloroplast stroma (m $s^{-1}$), respectively. We used an estimation of 0.0035 m $s^{-1}$ for the $g_{pl}$ and $g_{en}$ according to the previous studies[42,45], and estimated $g_{cw}$, $g_{ct}$ and $g_{st}$ using the formula of $g_i = \frac{r_f D_w p}{\Delta L_i}$ in the studies of Tomás *et al.*[26] and Niinemets and Reichstein (2003)[44], where $g_i$ (m $s^{-1}$) is either $g_{cw}$, $g_{ct}$ or $g_{st}$, $r_f$ is the dimensionless coefficient, $D_w$ ($m^2\ s^{-1}$) is the aqueous-phase volatile diffusion coefficient for $CO_2$ ($1.79 \times 10^{-9}$ $m^2\ s^{-1}$ at 25 °C), $\Delta L_i$ (m) is the diffusion path length, and $p$ ($m^3\ m^{-3}$) is the effective porosity. According to the previous studies of Tomás *et al.*[26] and Niinemets and Reichstein (2003)[44], $r_f$ was valued as 1 for cell wall, and an estimate of $r_f$ of 0.294 for $g_{ct}$ and $g_{st}$ in this study, $p$ was taken as 1 for $g_{ct}$ and $g_{st}$, and 0.3 for cell walls, $\Delta L_i$ was valued as $5.0 \times 10^{-7}$ (for cell wall, $\Delta L_{cw}$), $9.7 \times 10^{-8}$ (for cytosol, $\Delta L_{ct}$) and $1.65 \times 10^{-6}$ (for chloroplast stroma, $\Delta L_{st}$). $A_{mes}$ ($\mu m^2$) and $A_T$ ($\mu m^2$) are mesophyll surface area and total leaf surface area corrected for the actual area available for $CO_2$ diffusions, respectively, calculated from the light microscope.

**Measurement of leaf N content.** Leaves were picked and over-dried at 75 °C for 24 h to constant weight during gas exchange measuring periods and then ground using a mixer oscillating mill homogenizer (MM400, Retsch, Germany). Approximately 5.0 mg leaf samples were taken to measure leaf nitrogen content per area using a C N element analyser (Elementar vario MACRO, Element, Germany).

**Measurements of leaf aquaporin and carbonic anhydrase activities.** For analysing the physiological mechanism of $g_m$ and $g_{sc}$ responses to soil nitrogen additions, we sampled fifteen fresh leaves per treatment to measure the activities of aquaporin (AQP) and carbonic anhydrase (CA) using enzyme-linked immunosorbent assay (ELISA)[46,47]. Solid-phase antibody was made using purified plant AQP (or CA) antibody. Then, combined with antibody labelled with horseradish peroxidase (HRP), AQP (or CA) was added to microtiter plate wells to become an antibody-antigen-enzyme-antibody complex. This complex became blue with 3,3′,5,5′-tetramethyl benzidine (TMB) substrate solution after complete washing. The optical density (OD) values were measured spectrophotometrically at a wavelength of 450 nm to compare with the standard curves to determine the activity of AQP (or CA) in the samples.

**Statistical analysis.** SPSS 17.0 (SPSS Inc., Chicago, IL, USA) was used for one-way statistical analysis of normality and homogeneity of variance between nitrogen addition treatments (one-way ANOVA). Furthermore, regression analysis between $g_m$ and leaf N content was also performed. Mean values were compared using the least significant difference (LSD) multiple comparison test at the 0.05 and 0.01 probability levels ($P < 0.05$ and $P < 0.01$) with Tukey's honest significant difference (HSD) test.

## Data availability

All data analysed during this study are included in this published article and its Supplementary Information files.

Received: 13 February 2020; Accepted: 28 May 2020;
Published online: 22 June 2020

## References


1. Yamori, W., Nagai, T. & Makino, A. The rate-limiting step for $CO_2$ assimilation at different temperatures is influenced by the leaf nitrogen content in several $C_3$ crop species. *Plant. Cell Env.* **34**, 764–777 (2011).
2. Zhang, W. F. *et al*. Effect of nitrogen on canopy photosynthesis and yield formation in high-yielding cotton of Xinjiang. *Acta Agronomica Sin.* **28**, 789–796 (2002).
3. Wang, D., Yu, Z. W., Li, Y. Q., Shi, G. P. Effects of nitrogen fertilizer rate on photosynthetic character, sucrose synthesis in flag leaves and grain yield of strong gluten wheat Jimai 20. *Acta Agronomica Sinica* 903–908 (2007).
4. Holland, E. A., Dentener, F. J., Braswell, B. H. & Sulzman, J. M. Contemporary and pre-industrial global reactive nitrogen budget. *Biogeochemistry* **46**, 7–43 (1999).
5. Dore, M. H. I. Climate change and changes in global precipitation patterns: What do we know? *Environ. Int.* **31**, 1167–81 (2005).
6. Li, Y. *et al*. Light-saturated photosynthetic rate in high-nitrogen rice (*Oryza sativa* L.) leaves is related to chloroplastic $CO_2$ concentration. *J. Exp. Bot.* **8**, 2351–2360 (2009).
7. Li, Y. *et al*. Chloroplast downsizing under nitrate nutrition restrained mesophyll conductance and photosynthesis in rice (*Oryza sativa* L.) under drought conditions. *Plant. Cell Physiol.* **53**, 892–900 (2012).
8. Flexas, J. *et al*. Stomatal and mesophyll conductances to $CO_2$ in different plant groups: Underrated factors for predicting leaf photosynthesis responses to climate change? *Plant. Sci.* **226**, 41–48 (2014).
9. Centritto, M., Loreto, F. & Chartzoulakis, K. The use of low [$CO_2$] to estimate diffusional and non-diffusional limitations of photosynthetic capacity of salt-stressed olive sap lings. *Plant. Cell Env.* **26**, 585–594 (2003).
10. Flexas, J. *et al*. Mesophyll conductance to $CO_2$: current knowledge and future rospects. *Plant. Cell Env.* **31**, 602–621 (2008).
11. Oguchi, R., Hikosaka, K. & Hirose, T. Leaf anatomy as a constraint for photosynthetic acclimation: differential responses in leaf anatomy to increasing growth irradiance among three deciduous trees. *Plant. Cell Env.* **29**, 916–927 (2005).
12. Lundgren, C. Cell wall thickness and tangential and radial cell diameter of fertilized and irrigated Norway spruce. *Silva Fenn.* **38**, 95–106 (2004).
13. Muller, O. *et al*. The leaf anatomy of a broad-leaved evergreen allows an increase in leaf nitrogen content in winter. *Physiol. Plant.* **136**, 299–309 (2009).
14. Xiong, D. L. *et al*. Rapid responses of mesophyll conductance to changes of $CO_2$ concentration, temperature and irradiance are affected by N supplements in rice. *Plant. Cell Env.* **38**, 2541–2550 (2015).
15. Li, F. S., Kang, S. Z. & Zhang, J. H. Interactive effects of elevated $CO_2$, nitrogen and drought on leaf area, stomatal conductance, and evapotranspiration of wheat. *Agr. Water Manage.* **67**, 221–233 (2004).
16. Liu, Z. & Dickmann, D. I. Effects of water and nitrogen interaction on net photosynthesis, stomatal conductance, and water use-efficiency in two hybrid poplar clones. *Physiol. Plant.* **97**, 507–512 (2006).
17. Eller, F., Jensen, K. & Reisdorff, C. Nighttime stomatal conductance differs with nutrient availability in two temperate floodplain tree species. *Tree Physiol.* **37**, 428–440 (2017).
18. Kong, L. A., Xie, Y., Hu, L., Si, J. S. & Wang, Z. S. Excessive nitrogen application dampens antioxidant capacity and grain filling in wheat as revealed by metabolic and physiological analyses. *Sci. Rep.* **7**, 43363 (2017).
19. Sperling, O. *et al*. Excessive nitrogen impairs hydraulics, limits photosynthesis, and alters the metabolic composition of almond trees. *Plant. Physiol. Bioch* **143**, 265–274 (2019).
20. Wang, D., Xu, Z., Zhao, J., Wang, Y. & Yu, Z. Excessive nitrogen application decreases grain yield and increases nitrogen loss in a wheat-soil system. *Acta Agr. Scand. B – S. P* **61**, 681–692 (2011).
21. Miyazawa, S. I. *et al*. Deactivation of aquaporins decreases internal conductance to $CO_2$ diffusion in tobacco leaves grown under long-term drought. *Funct. Plant. Biol.* **35**, 553–564 (2008).
22. Uehlein, N. *et al*. Function of Nicotiana tabacum aquaporins as chloroplast gas pores challenges the concept of membrane $CO_2$ permeability. *Plant. Cell* **20**, 648–657 (2008).
23. Scafaro, A. P., Von Caemmerer, S., Evans, J. R. & Atwell, B. J. Temperature response of mesophyll conductance in cultivated and wild *Oryza* species with contrasting mesophyll cell wall thickness. *Plant. Cell Env.* **34**, 1999–2008 (2011).
24. Terashima, I., Hanba, Y. T., Tholen, D. & Niinemets, Ü. Leaf functional anatomy in relation to photosynthesis. *Plant. Physiol.* **155**, 108–116 (2011).
25. Peguero-Pina, J. J. *et al*. Leaf anatomical properties in relation to differences in mesophyll conductance to $CO_2$ and photosynthesis in two related Mediterranean *Abies* species. *Plant. Cell Env.* **35**, 2121–2129 (2012).
26. Tomás, M. *et al*. Importance of leaf anatomy in determining mesophyll diffusion conductance to $CO_2$ across species: quantitative limitations and scaling up by models. *J. Exp. Bot.* **64**, 2269–2281 (2013).
27. Muir, C. D., Hangarter, R. P., Moyle, L. C. & Davis, P. A. Morphological and anatomical determinants of mesophyll conductance in wild relatives of tomato (*Solanum sect. Lycopersicon, sect. Lycopersicoides; Solanaceae*). *Plant. Cell Env.* **37**, 1415–1426 (2014).
28. Perez-Martin, A. *et al*. Regulation of photosynthesis and stomatal and mesophyll conductance under water stress and recovery in olive trees: correlation with gene expression of carbonic anhydrase and aquaporins. *J. Exp. Bot.* **65**, 3143–3156 (2014).
29. Xiong, D. L. *et al*. Leaf anatomy mediates coordination of leaf hydraulic conductance and mesophyll conductance to $CO_2$ in *Oryza*. *N. Phytolo* **213**, 572–583 (2017).
30. Zhu, K. *et al*. Effects of soil rewatering on mesophyll and stomatal conductance and the associated mechanisms involving leaf anatomy and some physiological activities in Manchurian ash and Mongolian oak in the Changbai Mountains. *Plant. Physiol. Bioch* **144**, 22–34 (2019).
31. Xu, Z. Z. & Zhou, G. S. Responses of leaf stomatal density to water status and its relationship with photosynthesis in a grass. *J. Exp. Bot.* **59**, 3317–3325 (2008).
32. Uehlein, N., Lovisolo, C., Siefritz, F. & Kaldenhoff, R. The tobacco aquaporin NtAQP1 is a membrane $CO_2$ pore with physiological functions. *Nature* **425**, 734–737 (2003).
33. Flexas, J. *et al*. Keeping a positive carbon balance under adverse conditions: responses of photosynthesis and respiration to water stress. *Physiol. Plant.* **127**, 343–352 (2006).
34. Perez-Martin, A. *et al*. Physiological and genetic response of olive leaves to water stress and recovery: implications of mesophyll conductance and genetic expression of aquaporins and carbonic anhydrase. *Acta Horticulturae* **922**, 99–105 (2011).
35. Genty, B., Briantais, J. M. & Baker, N. R. The relationship between the quantum yield of photosynthetic electron-transport and quenching of chlorophyll fluorescence. *Biochimica et. Biophysica Acta* **990**, 87–92 (1989).
36. Valentini, R. *et al*. *In situ* estimation of net $CO_2$ assimilation, photosynthetic electron flow and photorespiration in Turkey oak (*Q. cerris* L.) leaves: diurnal cycles under different levels of water supply. *Plant. Cell Env.* **18**, 631–640 (1995).
37. Harley, P. C., Loreto, F., Marco, G. D. & Sharkey, T. D. Theoretical Considerations when Estimating the Mesophyll Conductance to $CO_2$ Flux by Analysis of the Response of Photosynthesis to $CO_2$. *Plant. Physiol.* **98**, 1429–1436 (1992).
38. Laisk, A. Kh. Kinetics of Photosynthesis and Photorespiration of $C_3$ Plants. *Mccarthy* (1977).
39. Walker, B. J., Skabelund, D. C., Busch, F. A. & Ort, D. R. An improved approach for measuring the impact of multiple $CO_2$ conductances on the apparent photorespiratory $CO_2$ compensation point through slope-intercept regression. *Plant. Cell Env.* **39**, 1198–1203 (2016).
40. Sun, J. W. *et al*. Day and night respiration of three tree species in a temperate forest of northeastern China. *iForest.* **8**, 25–32 (2015).
41. von Caemmerer, S. & Farquhar, G. D. Some relationships between the biochemistry of photosynthesis and the gas exchange of leaves. *Planta* **153**, 376–387 (1981).

42. Evans, J. R., von Caemmerer, S., Setchell, B. A. & Hudson, G. S. The relationship between $CO_2$ transfer conductance and leaf anatomy in tobacco transformed with a reduced content of Rubisco. *Aust. J. Plant. Physiol.* **21**, 475–495 (1994).
43. Thain, J. F. Curvature correction factors in the measurement of cell surface areas in plant tissues. *J. Exp. Bot.* **34**, 87–94 (1983).
44. Niinemets, Ü. & Reichstein, M. Controls on the emission of plant volatiles through stomata: a sensitivity analysis. *J. Geophys. Res.* **108**, 4211 (2003).
45. Tosens, T., Niinemets, U., Vislap, V., Eichelmann, H. & Castro, D. P. Developmental changes in mesophyll diffusion conductance and photosynthetic capacity under different light and water availabilities in *Populustremula*: how structure constrains function. *Plant. Cell Env.* **35**, 839–856 (2012).
46. Suárez, I., Salmerón-García, A., Cabeza, J., Capitán-Vallvey, L. F. & Navas, N. Development and use of specific ELISA methods for quantifying the biological activity of bevacizumab, cetuximab and trastuzumab in stability studies. *J. Chromatogr. B* **1032**, 155–164 (2016).
47. Grierson, C., Miller, D., LaPan, P. & Brady, J. Utility of combining MMP-9 enzyme-linked immunosorbent assay and MMP-9 activity assay data to monitor plasma enzyme specific activity. *Anal. Biochem.* **404**, 232–234 (2010).
48. Haupt-Herting, S., Klug, K. & Fock, H. P. A new approach to measure gross $CO_2$ fluxes in leaves. Gross $CO_2$ assimilation, photorespiration, and mitochondrial respiration in the light in tomato under drought stress. *Plant. Physiol.* **126**, 388–396 (2001).
49. Loreto, F., Delfine, S. & Di Marco, G. Estimation of photorespiratory carbon dioxide recycling during photosynthesis. *Funct. Plant. Biol.* **26**, 733–736 (1999).
50. Busch, F. A., Sage, T. L., Cousins, A. B. & Sage, R. F. $C_3$ plants enhance rates of photosynthesis by reassimilating photorespired and respired $CO_2$. *Plant. Cell Environ.* **36**, 200–212 (2013).
51. Tholen, D., Ethier, G., Genty, B., Pepin, S. & Zhu, X. G. Variable mesophyll conductance revisited: theoretical background and experimental implications. *Plant. Cell Env.* **35**, 2087–2103 (2012).
52. Evans, J. R. Nitrogen and photosynthesis in the flag leaf of wheat (*Triticum aestivum* L.). *Plant. Physiol.* **72**, 297–302 (1983).
53. Joha, R. E. Photosynthesis and nitrogen relationships in leaves of $C_3$ plants. *Oecologia* **78**, 9–19 (1989).
54. Makino, A., Nakano, H. & Mae, T. Responses of ribulose-1,5-bisphosphate carboxylase, cytochrome *f*, and sucrose synthesis enzymes to leaf nitrogen, and their relationships to photosynthesis. *Plant. Physiol.* **105**, 173–179 (1994).
55. Makino, A., Sato, T., Nakano, H. & Mae, T. Leaf photosynthesis, plant growth and nitrogen allocation in rice under different irradiances. *Planta* **203**, 390–398 (1997).
56. Xiong, D. L. *et al*. Leaf hydraulic conductance is coordinated with leaf morpho-anatomical traits and nitrogen status in the genus *Oryza*. *J. Exp. Bot.* **66**, 741–748 (2015).
57. Kaldenhoff, R. *et al*. Aquaporins and plant water balance. *Plant. Cell Env.* **31**, 658–666 (2008).
58. Clarkson, D. T. *et al*. Root hydraulic conductance: Diurnal aquaporin expression and the effects of nutrient stress. *J. Exp. Bot.* **51**, 61–70 (2000).
59. Hacke, U. G. *et al*. Influence of nitrogen fertilization on xylem traits and aquaporin expression in stems of hybrid poplar. *Tree Physiol.* **30**, 1016–1025 (2010).
60. Flexas, J. *et al*. Tobacco aquaporin *Nt*AQP1 is involved in mesophyll conductance to $CO_2$ *in vivo*. *Plant. J.* **48**, 427–439 (2006).
61. Chartzoulakis, K., Patakas, A. & Kofidis, G. Water stress affects leaf anatomy, gas exchange, water relations and growth of two avocado cultivars. *Sci. Hortic-Amsterdam* **95**, 39–50 (2002).
62. Onoda, Y. *et al*. Physiological and structural tradeoffs underlying the leaf economics spectrum. *N. Phytol.* **214**, 1447–1463 (2017).
63. Han, J. M. *et al*. Mesophyll conductance in cotton bracts: anatomically determined internal $CO_2$ diffusion constraints on photosynthesis. *J. Exp. Bot.* **69**, 5433–5443 (2018).
64. Hanba, Y. T. *et al*. Overexpression of the barley aquaporin HvPIP 2;1 increases internal $CO_2$ conductance and $CO_2$ assimilation in the leaves of transgenic rice plants. *Plant. Cell Physiol.* **45**, 521–529 (2004).
65. Peguero-Pina, J. J. *et al*. Leaf morphological and physiological adaptations of a deciduous oak (*Quercus faginea* Lam.) to the Mediterranean climate: a comparison with a closely related temperate species (*Quercus robur* L.). *Tree Physiol.* **36**, 287–299 (2016).
66. Nadal, M., Flexas, J. & Gulías, J. Possible link between photosynthesis and leaf modulus of elasticity among vascular plants: a new player in leaf traits relationships? *Ecol. Lett.* (2018).
67. Nadal, M. & Flexas, J. Variation in photosynthetic characteristics with growth form in a water-limited scenario: Implications for assimilation rates and water use efficiency in crops. *Agr. Water Manage.* **216**, 457–472 (2019).
68. Laza, R. C., Bergman, B. & Vergara, B. S. Cultivar differences in growth and chloroplast ultrastructure in rice as affected by nitrogen. *J. Exp. Bot.* **44**, 1643–1648 (1993).


## Acknowledgements

This study was partially supported by the National Natural Science Foundation of China (Grant No. 41975150, 41675112, 31670707, 31870625) and Liaoning Provincial Natural Science Foundation (2020-MS-027). We acknowledged Prof. Jaume Flexas Sans from Universitat de les Illes Balears and two anonymous reviewers for their helpful comments and suggestions on this manuscript. We were grateful to the National Research Station of Changbai Mountain Forest Ecosystems of the Chinese Academy of Sciences Authority for permission to collect soil samples from the Korean Pine experimental Forest. We thanked the support and technical assistance from the research group of Eco-climatology, Institute of Applied Ecology, CAS.

## Author contributions

F.Y., D.G. and C.J. conceived the project. K.Z., A.W. and Y.Z. performed the field experiments. K.Z., C.G. and J.W. contributed to lab work. K.Z., A.W. and J.W. interpreted the results. K.Z., F.Y. and D.G. wrote the manuscript with assistance from other coauthors.

## Competing interests

The authors declare no competing interests.

## Additional information

**Supplementary information** is available for this paper at https://doi.org/10.1038/s41598-020-66886-x.

**Correspondence** and requests for materials should be addressed to F.Y. or D.G.

**Reprints and permissions information** is available at www.nature.com/reprints.